

Contribution to the theory of an ionizing shock wave in a transverse magnetic field

L. A. Velikovich and M. A. Liberman

Institute of Physics Problems, USSR Academy of Sciences, Physics Laboratory
(Submitted March 28, 1977)

Zh. Eksp. Teor. Fiz. 73, 891-912 (September 1977)

The structure of the front of a strong ionizing shock wave propagating in a gas transversely to a magnetic field is determined. This structure depends on the wave intensity. At contemporary shock-wave intensities, the wave front splits into a heating zone and an ionization zone. The heating zone is then determined by the ohmic dissipations. At Mach numbers above critical, however, the smooth variations of the temperature and of the density give way to a discontinuity (isomagnetic jump) in the Joule heating region. In this discontinuity, at a constant magnetic field, all the remaining quantities change as a result of viscosity and thermal conductivity. In the relaxation zone the gas becomes ionized, the temperature drops, and the density and the magnetic field increase, the magnetic field being frozen into the relaxation zone. The structure of a higher-intensity shock wave does not split into a heating and an ionization zone, but even in this case, an isomagnetic jump appears on the shock-wave front at Mach numbers higher than critical. The boundary conditions and the shock adiabats are calculated with account taken of the dissociation and the multiple ionization. The question of the boundary conditions ahead of the ionizing shock wave front in a magnetic field is discussed. It is shown that under certain conditions the precursor photoionization can exert a decisive influence on the observed magnetic structure of the front. The results are compared with the available experimental data. It is shown that allowance for a shock-wave structure with an isomagnetic jump eliminates the contradiction between the theory [Kulikovskii and Lyubimov, *Sov. Phys. Doklady* 4, 1195 (1960); C. K. Chu, *Phys. Fluids* 7, 1349 (1964)] and the experimentally measured electric and magnetic fields behind the wave front [C. F. Stebbins and G. C. Vlases, *J. Plasma Phys.* 2, 633, 1968].

PACS numbers: 47.40.Nm

INTRODUCTION

It is known that the temperature of a gas behind the front of a strong shock wave propagating through an initially neutral gas becomes high enough to ionize the gas behind the shock wave. An essential role is then assumed by the interaction of the shock wave with the electromagnetic field. The study of ionizing shock waves is necessary both for the interpretation of laboratory experiments (electromagnetic shock tubes, pinches, and others) and for astrophysical requirements. References to the experimental and theoretical papers can be found in the reviews of Chu and Gross.^[1,2]

We solve in this paper the problem of the structure of the front of an ionizing shock wave propagating in a gas across a magnetic field. For all the gas-density values of practical interest, the main dissipative processes are the Joule processes, which in fact determine the width of the shock-wave front. But at Alfvén Mach numbers exceeding the critical values, the Joule dissipation is insufficient for a continuous passage through the shock front. A discontinuity—*isomagnetic jump*^[3]—then appears in the structure of the front. At a constant magnetic field, the pressure, the temperature, and the gas density become discontinuous in the *isomagnetic jump*.

Depending on the ratio of the shock-wave intensity to the gas density, the rate of ionization on the shock-wave front can be either much lower or larger than the rate of change of the state of the gas. In the former case the *isomagnetic jump* gives way to an ionization zone

that is much broader than the heating zone. In the ionization zone, the gas becomes ionized and cooled, but the total pressure and the density increase monotonically. The magnetic field, being frozen-in, increases slowly in this zone and reaches its equilibrium value. This situation, with a distinct separation of the heating and reaction zones in the shock wave, is analogous to the well-known detonation model of Zel'dovich and von Neumann. A situation is also possible in which the ionization rate on the front becomes very rapidly larger than the rate of change of the state of the gas. Then the shock-wave front is no longer divided into a heating zone and an ionization zone—the ionization, which is practically in equilibrium, proceeds simultaneously with the heating, and the degree of ionization is determined by the Saha formula. If the Alfvén Mach number is larger than critical in this case, then the produced *isomagnetic jump* is located at the end of the shock front.

The front of the ionizing shock wave is always preceded by preceding (precursor) ionization, which is produced in this case mainly on account of the photoionization due to the light quanta coming from the heated gas region behind the shock-wave front. The precursor ionization must be taken into account both in the formulation of the correct boundaries and for the interpretation of the experimental results,^[4] since the magnitude of the precursor ionization determines whether the characteristic length of the Joule dissipations, i. e., the dimension over which the magnetic field changes, is much smaller or much larger than the dimensions of the apparatus. The magnitude of the precursor ion-

ization thus determined the gradient of the variation of the magnetic field and the position of the isomagnetic jump.

Although we shall deal hereafter mainly with shock waves in argon, all the results have a character common to all gases. The actual calculations and the comparison with experiments are carried out for argon and hydrogen.^[4-6]

1. FORMULATION OF PROBLEM. INITIAL EQUATIONS

Consider a plane stationary shock wave propagating with velocity u_1 in an immobile neutral gas along the x axis, in a direction perpendicular to a magnetic field H aligned with the z axis. In a coordinate frame that moves together with the shock-wave front we have a stationary stream of neutral gas that flows in at velocity u_1 from $x = -\infty$ (state 1) into the front, and an ionized gas, that flows out to $x = +\infty$ (state 2).

For the y component of the electric field we get from the equation $\text{curl } \mathbf{E} = 0$ that $dE_y/dx = 0$, whence $E_{y1} = E_{y2} = \text{const}$ (the subscripts 1 and 2 denote throughout the equilibrium values of quantities in the state 1 or 2). From the equation

$$\text{rot } \mathbf{H} = 4\pi \mathbf{j}/c$$

and from Ohm's law $\mathbf{j} = \sigma(\mathbf{E} + \mathbf{v} \times \mathbf{H}/c)$ we have

$$\frac{dH}{dx} = \frac{4\pi\sigma}{c} \left(\frac{vH}{c} - E_y \right),$$

where σ is the conductivity of the gas.

In the equilibrium states 1 and 2, i. e., far ahead or behind the shock-wave front, all the gradients vanish. Thus, writing down the last equation for state 2, we get $E_{y2} = u_2 H_2/c$. At the same time, in the case when there is no conductivity in front of the shock wave ($\sigma_1 = 0$), there is no analogous connection between E_{y1} and H_1 . It follows therefore that the value of E_{y1} in front of the shock wave can be specified arbitrarily as a supplementary condition. This was first pointed out in^[7]. For example, at $E_{y1} = 0$ we have $H_2 = 0$, and at $E_{y1} = u_2 H_1/c$ the magnetic field does not change at all on going through the shock-wave front: $H_2 = H_1$. Actually, as shown by a more detailed analysis^[8], the value of E_{y1} is not arbitrary, but depends on the structure of the shock-wave front.^[1]

It is obvious that the problem connected with the supplementary conditions for E_{y1} is based on the assumption that the equality $\sigma_1 = 0$ is exact. By specifying an arbitrary albeit small value $\sigma_1 \neq 0$ as $x \rightarrow -\infty$ we get the usual magnetohydrodynamic condition $E_{y1} = u_1 H_1/c$. It is also obvious that results having a physical meaning must not depend on the assumption $\sigma_1 = 0$ as $x \rightarrow -\infty$ or $\sigma_1 \rightarrow 0$ as $x \rightarrow -\infty$.

We shall return to this question later in connection with the discussion of the experiments of Stebbins and Vlasov.^[4] For the time being we choose as the boundary condition

$$E_{y1} = u_1 H_1/c.$$

This is justified by the already mentioned fact that the front of a strong shock wave is always preceded by a broad region of pre-ionized gas—the precursor zone.^[9-10] For example, in argon in front of a shock wave the observed^[11] degree of ionization is $\alpha_1 \sim 10^{-5} - 10^{-8}$ over a length on the order of several dozen centimeters (in a pressure range from 10^{-2} to 1 Torr).

We assume the plasma to be quasineutral throughout, putting $n_i = n_e = n$; this is equivalent to assuming a small Debye radius compared with the characteristic lengths of the problem. Then, taking into account the smallness of the y component of the ion velocity in comparison with the electron velocity v_y^e , we obtain^[3]

$$\frac{dH}{dx} = \frac{4\pi}{c} n e v_y^e. \quad (1.1)$$

From the vanishing of the x component of the current it follows that $v_x^e = v_x^i = v$.

To investigate the structure of an ionizing shock wave, we shall use the equations of multicomponent hydrodynamics for electrons, ions, and neutral atoms, with account taken of the inelastic ionization and recombination processes. Owing to the precursor ionization, the degree of ionization on the front of the shock wave is large enough, so that we can neglect the ionization due to atom-atom collisions in comparison with the ionization by electron impact. The inverse process—recombination—is insignificant practically everywhere on the shock-wave front, and comes into play far behind the front, in the region where ionization equilibrium is established (in this case we already have $T_e \approx T_i$). For the sake of argument we assume that three-particle recombination takes place. Then, designating by n and N_a the densities of the electrons and of the neutral atoms, we write the balance equation for the number of particles in the form

$$d(nv)/dx = \dot{n} = \alpha_{ion} n N_a - \beta_{rec} n^3. \quad (1.2)$$

In the region behind the shock-wave front ($x \rightarrow +\infty$) the plasma is in equilibrium and has $T = T_e = T_a$. Then $\dot{n} = 0$ and the electron density is determined by the Saha formula

$$n^2 = \frac{g_e g_i}{g_a} N_a \left(\frac{m_e T_e}{2\pi \hbar^2} \right)^{3/2} \exp\left(-\frac{I}{T_e}\right). \quad (1.3)$$

It is known that in inert gas the ionization proceeds in many steps. The ionization coefficient of argon is given by^[12]

$$\alpha_{ion} = C^* (8T_e/\pi m_e)^{3/2} (I_1^* + 2T_e) \exp(-I_1^*/T_e),$$

where $I_1^* = 11.5$ eV is the excitation potential, and the quantity $C^* = 7 \times 10^{-18}$ cm²/eV is defined in^[5]. For the recombination coefficient we must assume the value

$$\beta_{rec} = C^* \frac{g_a}{g_e g_i} \frac{8\pi \hbar^3}{m_e^2} \left(\frac{I}{T_e} + 2 \right) \exp\left(\frac{I}{T_e} - \frac{I_1^*}{T_e} \right),$$

which agrees well with the experimentally measured values at temperatures higher than 0.5 eV.

The continuity, motion, and energy-transport equations for each plasma component (electrons, ions, and neutral atoms) are obtained by integrating the corresponding moments of the kinetic equation, where the collision integral takes into account, besides the elastic collisions, the impact ionization and the recombination. The system of equations obtained in this manner is quite cumbersome, and without presenting all of it here, we use immediately some simplifications.

We note that charge-exchange processes make the cross section σ_{ia} of the ion-atom collisions large, and therefore the ions slip past the atoms, i.e., $\mathbf{v}_i = \mathbf{v}_a$. For argon we have^[13,14] $\sigma_{ia} = 1.4 \times 10^{-14} \text{ cm}^2$, which is larger by approximately one order of magnitude than the atom-atom collision cross section $\sigma_{aa} = 1.7 \times 10^{-14} T_a^{-1/4} \text{ cm}^2$. Neglecting the mass difference between the ions and the atoms we conclude in similar fashion that their temperatures are also equal, $T_i = T_a = T$.

It was also shown in^[3] that the electron viscosity and thermal diffusion can also be neglected. Putting $m_i = m_a = M$, we write $\varepsilon = (m_e/M)^{1/2} \ll 1$, ($\varepsilon = 3.6 \times 10^{-3}$ for argon). Taking all the simplifications into account and neglecting terms small in ε , we obtain the following initial equations.

Adding and integrating the continuity equations for the electrons and atoms, we have

$$Nv = C, \quad (1.4)$$

where $N = n + N_a$. The integral of the momentum transport equation of the plasma as a whole (electrons, ions, and atoms), takes the form

$$MNv^2 + nT_e + NT + H^2/8\pi + \pi_{xx}^i + \pi_{xx}^a = P, \quad (1.5)$$

where π^i and π^a are the tensors of the viscous stresses of the ion and neutral components. The integral of the energy-transport equation for the gas as a whole is

$$\begin{aligned} & \frac{1}{2}MNv^3 + \frac{3}{2}NTv + \frac{5}{2}nT_e v + (\pi_{xx}^i + \pi_{xx}^a)v \\ & + q_x^i + q_x^e + q_x^a + cE/H/4\pi + Inv = S. \end{aligned} \quad (1.6)$$

Here q^e , q^i , and q^a are the heat fluxes of the electrons, ions, and atoms; C , P , and S in Eqs. (1.4)–(1.6) are integration constants determined by the boundary conditions. Neglecting the inertia of the electrons (see^[3]), we write down the equation of motion of the electrons along the y axis:

$$en(E_y - vH/c) = R_y^e. \quad (1.7)$$

Finally, the heat-transfer equation for the heavy plasma component (the atoms together with the ions) are

$$\frac{3}{2}Nv \frac{dT}{dx} + NT \frac{dv}{dx} + (\pi_{xx}^i + \pi_{xx}^a) \frac{dv}{dx} + \frac{d}{dx}(q_x^i + q_x^a) = Q_{ie} + Q_{ae}. \quad (1.8)$$

Here R_y^e is the y -component of the friction force due to the collisions of the electrons with the atoms and ions, while Q_{ie} and Q_{ae} are the amounts of heat transferred in

the collisions of the heavy particles with the electrons.

Equations (1.1), (1.2), and (1.4)–(1.8) constitute the complete system of equations for the variables N , $\alpha = n/N$, v , v_y^e , T , T_e , and H . Their solution determines in principle the shock-wave structure. The forms of the kinetic coefficients, of the friction force, and of the terms connected with heat exchange are well known in the case of elastic collisions.^[15,16]

We determine the frequency of the collisions of the particles of sort α in the following manner²⁾:

$$\nu_\alpha = \sum_\beta 2\mu_{\alpha\beta} N_\beta \sigma_{\alpha\beta} v_{\alpha\beta},$$

where $\mu_{\alpha\beta} = m_\alpha m_\beta / (m_\alpha + m_\beta)$ is the reduced mass, N_β is the density of particles of sort β , $\sigma_{\alpha\beta}$ is the cross section for the collisions of particles α and β , and $v_{\alpha\beta}$ is the relative thermal velocity of particles α and β . We denote the Coulomb cross section by $\sigma_c = \sigma_{ei} = \sigma_{ee} = \pi e^4 \Lambda / 2T_e^2$. Then, accurate to terms small in ε , we have for the frequencies of the collisions of the electrons, ions, and atoms the following expressions:

$$\begin{aligned} \nu_e &= (8T_e/\pi m_e)^{1/2} [2N_a \sigma_{ea} + (2 + \sqrt{2})n\sigma_c], \\ \nu_i &= (16T/\pi M)^{1/2} [N_a \sigma_{ia} + n\sigma_c (T_e/T)^2], \\ \nu_a &= (16T/\pi M)^{1/2} [N_a \sigma_{aa} + n\sigma_{ia}]. \end{aligned}$$

For the viscous-stress tensor we have

$$\pi_{xx}^{i,a} = -\frac{1}{3} \eta^{i,a} dv/dx,$$

where the viscosity coefficients are

$$\eta^{i,a} = \frac{5}{3} N_{i,a} T / \nu_{i,a}.$$

Since there is no slipping, there are no drift terms in the heat fluxes, in the friction forces, and in the terms with heat exchange Q_{ea} and Q_{ei} . Then the heat flux will be $q_x = \kappa dT/dx$. The heat conduction coefficients for the electrons, ions, and atoms are

$$\kappa_e = \frac{75}{16} \frac{nT_e}{m_e v_e}, \quad \kappa_i = \frac{75}{16} \frac{nT}{M v_i}, \quad \kappa_a = \frac{75}{16} \frac{N_a T}{M v_a}.$$

The friction force of the electrons colliding with the atoms and ions is

$$R_y^e = -\frac{2}{3} m_e n v_y^e (v_{ea} + v_{ei}).$$

The heat transferred in the elastic collisions of the heavy particles with the electrons is equal to

$$Q_{ie} = -\frac{2m_e}{M} n v_{ei} (T - T_e), \quad Q_{ae} = -\frac{2m_e}{M} n v_{ea} (T - T_e)$$

(the corresponding contribution of the inelastic collisions is the term Inv in (1.6)).

The values of the elastic cross section for the scattering of an electron by argon atoms are shown in^[14] and can be represented for $T \lesssim 6-7$ eV in the form³⁾

$$\sigma_{ea}(T_e) = \left\{ 0.2 + 2.7T_e - \frac{0.27}{(4T_e + 1)^{1/2}} [311T_e^2 - 32T_e - 4] \right\} \cdot 10^{-16} \text{ cm}^2$$

where T_e is in electron volts.

We note that in the expression for R_e^* , we can disregard the inelastic collisions, since the frequency of the inelastic collisions that lead to a change in the electron momentum is much lower than the frequency of the elastic collisions. For the same reason, the contribution of the inelastic collisions to the viscosity coefficient is small. Allowance for the inelastic collisions for the thermal-conductivity coefficient leads to a non-monotonic temperature dependence of κ_e . In the region $T \sim 0.1J$, where J is the dissociation or ionization energy, κ_e has a sharp maximum. But since the integrated contribution of the thermal conductivity is significant for the structure of the shock front, that part of the thermal-conductivity coefficient which is connected with the transport of the inelastic energy (of dissociation and ionization) can be disregarded in the first order approximation.

2. DIMENSIONLESS EQUATIONS. BOUNDARY CONDITIONS. SHOCK ADIABAT

To investigate Eqs. (1.1)–(1.8) it is convenient to change over to dimensionless variables, which are defined as the ratios of the quantities (temperature, density, etc.) to the corresponding equilibrium values in states 1 or 2. Recognizing that the concentration $\alpha = n/N$ is already dimensionless, we define the following dimensionless variables:

$$\begin{aligned} \omega &= v/u_1, \quad \Theta = T/T_1, \quad \Theta_e = T_e/T_1, \\ v &= N/N_1, \quad h = H/H_1, \quad \zeta = x/\Delta. \end{aligned} \quad (2.1)$$

The choice of the scale of the coordinate Δ is governed by physical considerations and is described in detail in our preceding paper.^[3]

We introduce the acoustic and Alfvén Mach numbers:

$$M^2 = Mu^2/\gamma(1+\alpha)T, \quad M_a^2 = 4\pi NMu^2/H^2.$$

Unless otherwise stipulated, we consider hereafter a simple gas with an adiabatic exponent $\gamma = 5/3$. The continuity equation in dimensionless variables is

$$v\omega = 1. \quad (2.2)$$

We eliminate v from (1.1)–(1.8) with the aid of (1.7) and change to dimensionless variables. Substituting $v = 1/\omega$, we obtain the following equations:

$$\frac{d\alpha}{d\zeta} = \alpha(1-\alpha) \frac{\Delta}{\Delta_{ion}} - \alpha^3 \frac{\Delta}{\Delta_{rec}}, \quad (2.3)$$

$$h\omega - 1 = \frac{\Delta_j dh}{\Delta d\zeta} \quad (2.4)$$

$$\begin{aligned} \omega - 1 + \frac{3}{5M_1^2(1+\alpha_1)} \left(\frac{\Theta}{\omega} - 1 + \alpha \frac{\Theta_e}{\omega} - \alpha_1 \right) \\ + \frac{h^2 - 1}{2M_{a1}^2} - \frac{\Delta_j d\omega}{\Delta d\zeta} = 0, \end{aligned} \quad (2.5)$$

$$\omega^2 - 1 + \frac{3}{M_1^2(1+\alpha_1)} (\Theta + \alpha\Theta_e - 1 - \alpha_1) + 2 \frac{h-1}{M_{a1}^2}$$

$$+ \frac{6\Theta_1^{ion}}{5M_1^2(1+\alpha_1)} (\alpha - \alpha_1) - 2 \frac{\Delta_v}{\Delta} \omega \frac{d\omega}{d\zeta} - 2 \frac{\Delta_{re}}{\Delta} \frac{d\Theta_e}{d\zeta} - 2 \frac{\Delta_r}{\Delta} \frac{d\Theta}{d\zeta} = 0, \quad (2.6)$$

$$\begin{aligned} \frac{d\Theta}{d\zeta} + \frac{2}{3} \frac{\Theta}{\omega} \frac{d\omega}{d\zeta} + \frac{5M_1^2}{3} (1+\alpha_1) \frac{\Delta_v}{\Delta} \left(\frac{d\omega}{d\zeta} \right)^2 \\ - \frac{5M_1^2}{3} (1+\alpha_1) \frac{d}{d\zeta} \frac{\Delta_r}{\Delta} \frac{d\Theta}{d\zeta} + \frac{\Delta}{\Delta_r} (\Theta - \Theta_e) = 0. \end{aligned} \quad (2.7)$$

In (2.3)–(2.7), the quantities Δ_{ion} , Δ_{rec} , Δ_v , Δ_{Te} , Δ_T , Δ_j , and Δ_r , with the dimension of length, are the scale characterizing respectively the processes of ionization, recombination, viscosity, electronic thermal conductivity, and heat conduction of the heavy component, the Joule dissipations, and the temperature relaxation. Denoting by l_e , l_a , and l_i the electron, atom, and ion mean free paths, we have

$$\begin{aligned} \Delta_v &= \Delta_{vi} + \Delta_{ve} = \left(\frac{5\pi}{24} \right)^{1/2} \frac{\Theta^{1/2}}{\omega M_1} (\alpha l_i + (1-\alpha) l_e) \\ \Delta_{re} &= \frac{27}{16\epsilon M_1^3} \left(\frac{5\pi}{24} \right)^{1/2} \frac{\alpha}{\omega} \Theta_e^{1/2} l_e, \\ \Delta_r &= \frac{27}{16M_1^3} \left(\frac{5\pi}{24} \right)^{1/2} \frac{\Theta^{1/2}}{\omega} [\alpha l_i + (1-\alpha) l_a], \\ \Delta_j &= \frac{c^2}{4\pi\sigma u_1} = \left(\frac{8}{15\pi^2} \right)^{1/2} \frac{\Theta^{1/2}}{\epsilon M_1 r_e} \left[\sigma_K + \left(\frac{1}{\alpha} - 1 \right) \sigma_{ee} \right], \\ \Delta_r &= \frac{M_1}{4\epsilon} \left(\frac{5\pi}{24} \right)^{1/2} \alpha^{-1} \omega^2 \Theta^{-1/2} [(1-\alpha) \sigma_{ea} + \alpha \sigma_{K}]^{-1}, \\ \Delta_{ion} &= \omega^2 u_1 / \alpha_{ion} N_1, \quad \Delta_{rec} = \omega^2 u_1 / \beta_{rec} N_1^2, \end{aligned}$$

where $r_e = e^2/m_e c^2 = 2.82 \cdot 10^{-13}$ cm.

As already mentioned, the choice of the scale for making the coordinates dimensionless is determined by physical considerations. In particular, over Δ scales much larger than the scales of the listed processes, the shock wave constitutes a discontinuity that has no structure. Putting $\Delta = \infty$ in Eqs. (2.3)–(2.7), we obtain algebraic equations that represent the conservation laws that connect the quantities ahead and behind the shock-wave front. The degree of ionization α_2 has here the equilibrium value given by the Saha formula with temperature T_2 , while $\alpha_1 \ll 1$ can also be the non-equilibrium priming ionization in the precursor zone, produced, say, by photoionization:

$$\omega - 1 + \frac{3}{5M_1^2(1+\alpha_1)} \left[\frac{\Theta}{\omega} (1+\alpha_2) - 1 - \alpha_1 \right] + \frac{h^2 - 1}{2M_{a1}^2} = 0, \quad (2.8)$$

$$\begin{aligned} \omega^2 - 1 + \frac{3}{M_1^2(1+\alpha_1)} [\Theta(1+\alpha_2) - 1 - \alpha_1] + 2 \frac{h-1}{M_{a1}^2} \\ + \frac{6\Theta_1^{ion}}{5M_1^2(1+\alpha_1)} (\alpha_2 - \alpha_1) = 0, \end{aligned} \quad (2.9)$$

$$h\omega - 1 = 0. \quad (2.10)$$

Here $\Theta_1^{ion} = I/T_1$ is the dimensionless ionization potential.

It is obvious that in the case of a weak shock wave, when the ionization loss is small ($\alpha_2 \ll T_2/I$), just as in the case of a very strong shock wave with a temperature $T_2 \gg I$ behind the front, the last term in (2.9) is immaterial. The Hugoniot relations then become the same as for a transverse shock wave in a plasma.^[3,9] We then have for the velocity and temperature discontinuities across the shock-wave front, omitting the last term of (2.9)

$$\omega_{02} = \frac{1}{8} \left\{ 1 + \frac{3}{M_1^2} + \frac{5}{2M_{a1}^2} + \left[\left(1 + \frac{3}{M_1^2} + \frac{5}{2M_{a1}^2} \right)^2 + \frac{8}{M_{a1}^2} \right]^{1/2} \right\}, \quad (2.11)$$

$$2\Theta_{02} = \frac{2T_{02}}{T_1} = 1 + \frac{M_1^2}{3\omega_{02}} (1 - \omega_{02}) \left(\omega_{02}^2 + \omega_{02} - \frac{2}{M_{a1}^2} \right). \quad (2.12)$$

As seen from (2.11), the maximum compression in the maximally strong shock wave is $N_2/N_1 = 1/\omega_{02} = 4$. In the case of argon, this is not at all the case, since the ionization potentials of the first argon shell are quite close to one another ($I_1 = 15.7$ eV, $I_2 = 27.6$ eV, $I_3 = 40.9$ eV, etc.) and make an appreciable contribution to the shock-wave energy balance in the entire range of the presently attainable Mach numbers.^[2]

Neglecting α_1 in comparison with unity, we get from (2.9)

$$\Theta_2 = (\Theta_{02}(\omega_2)^{-2} \alpha_2 \Theta_1^{\text{ion}}) / (1 + \alpha_2), \quad (2.13)$$

Θ_{02} is the maximum value of the temperature reached on the front of the ionizing shock wave. From (2.8) and (2.9) we get

$$(\omega - 1)(\omega - \omega_{02})(\omega - \omega_{02-}) = \frac{1}{10} \Theta_1^{\text{ion}} \alpha_2 / M_1^2, \quad (2.14)$$

where the expression for ω_{02-} differs from (2.11) for ω_{02} in the sign in front of the square root.

We write in (2.14) $\Theta_1^{\text{ion}} = I/T_1 = I\Theta_2/T_2 = \Theta_2^{\text{ion}}\Theta_2$ and substitute Θ_2 from (2.8). Then, omitting terms shall in comparison with $1/M_1^2$, we obtain the following expression for the jump of the discontinuity through the shock-wave front:

$$\omega_2 = \frac{1}{8(\kappa+1)} \left\{ 1 + \frac{3}{M_1^2} + \frac{5+4\kappa}{2M_{a1}^2} + \left[\left(1 + \frac{3}{M_1^2} + \frac{5+4\kappa}{2M_{a1}^2} \right)^2 + \frac{8(\kappa+1)(4\kappa+1)}{M_{a1}^2} \right]^{1/2} \right\}. \quad (2.15)$$

The parameter $\kappa = \alpha_2 \Theta_2^{\text{ion}} / 2(1 + \alpha_2)$ characterizes here the influence of the ionization on the velocity jump and the compression $\nu_2/1\omega_2$ in the shock wave. In the limit of an infinitely strong ($T_2 \rightarrow \infty$, $\Theta_2^{\text{ion}} \rightarrow 0$) or weak ($\alpha_2 \rightarrow 0$) shock wave we have $\omega_2 \rightarrow \omega_{02}$. It is also seen from (2.15) that when the gas density is decreased κ increases without limit; consequently the compression and the velocity jump in the ionizing shock wave can become in principle arbitrarily large. From (2.8)–(2.10) we obtain the equation of the shock adiabat:

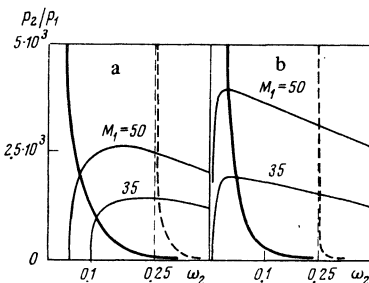


FIG. 1. Shock adiabats for argon ($N_1 = 10^{16}$ cm⁻³, $T_1 = 300$ K) at $\beta_1 = 0.1$ (a) and $\beta_1 = 10$ (thick curves). The thin curves are plots of (2.17).

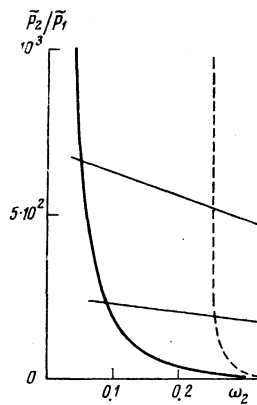


FIG. 2. Shock adiabat of argon, $N_1 = 10^{16}$ cm⁻³, $T_1 = 300$ K, $\beta_1 = 0.1$; thin lines—plots of (2.17a).

$$\frac{p_2}{p_1} = \left(\frac{1 + \alpha_1}{1 + \alpha_2} \right) \frac{1}{4\omega_2 - 1} \left[4 - \omega_2 + \frac{(1 - \omega_2)^3}{\beta_1 \omega_2} - 2\Theta_1^{\text{ion}} \frac{\alpha_2 - \alpha_1}{1 - \alpha_1} \right], \quad (2.16)$$

where

$$\omega_2 = u_2/u_1 = N_1/N_2, \quad \beta_1 = 8\pi N_1 T_1 / H_1^2.$$

In the case when ionization can be neglected, Eq. (2.16) goes over into the equation of the shock adiabat of a fully ionized plasma.^[9] In the general case (2.16) is an implicit equation for the shock adiabat. Figure 1 shows the shock adiabats with ionization, while the dashed curves show the shock adiabats with ionization not taken into account (more accurately, with quenched ionization). If the shock wave is not too intense, its front can be subdivided into a compression (heating) zone and into a relaxation (ionization) zone. The dashed curve in Fig. 1a is then the shock adiabat for the shock wave of the compression zone. From the continuity and momentum-conservation equations we obtain

$$p_2 - p_1 = \rho_1 u_1^2 (1 - \omega_2) \left[1 - (\omega_2 + 1) / 2\omega_2^2 M_{a1}^2 \right]. \quad (2.17)$$

The intersection of the curve (2.17) with the shock adiabat (Fig. 1a) yields the pressure at a given shock-wave velocity u_1 . As seen from Fig. 1, the gas pressure in the relaxation zone can be larger as well as smaller than the pressure in the compression zone. The reason is the decrease of the temperature in the relaxation zone, because energy is lost to ionization. The total pressure $p = p + H^2/8\pi$ through the shock-wave front, however, always increases monotonically. We have

$$\tilde{p}_2 - \tilde{p}_1 = \rho_1 u_1^2 (1 - \omega_2) \quad (2.17a)$$

—the thin lines in Fig. 2. We see that $\tilde{p}_2 > \tilde{p}_{02}$ always. Although we are not dealing in the present paper with the kinetics of multiple ionization (or ionization and dissociation in the case of hydrogen), these effects must be taken into account when the boundary conditions are written out. In the case of a shock wave propagating we put n_{H_2} , n_H and $n = n_i = n_e$ for the respective densities of the hydrogen molecules, atoms, and ions. We introduce $N = n + n_H + 2n_{H_2}$, the degree of dissociation $\eta = (n$

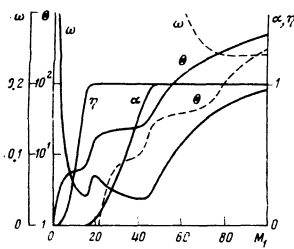


FIG. 3. Dimensionless temperature Θ , velocity ω , degree of dissociation η , and degree of ionization α as functions of the Mach number M_1 in a shock wave in hydrogen at $T_1=300$ K. Solid line— $p_1=1.5 \times 10^{-6}$ Torr and $\beta_1=8.8$; dashed line— $p_1=0.1$ Torr, $\beta_1=3 \times 10^{-3}$.

+ n_H)/ N , and the degree of ionization $\alpha=n/M$. We recognize that

$$\gamma_{H_2}=(7+2c_{vib})/(5+2c_{vib}),$$

where

$$c_{vib}=(\Theta_{vib}/\Theta)^2 \exp(\Theta_{vib}/\Theta) [\exp(\Theta_{vib}/\Theta)-1]^{-2}$$

is the vibrational part of the specific heat (for H_2 we have $\Theta_{vib}=\hbar\Omega/kT_1=6100$ K/ T_1). The momentum and energy conservation equations take in the dimensionless variables the form

$$\omega-1+\frac{\hbar^2-1}{2M_{a1}^2}+\frac{5}{7M_1^2} \left[(1+\eta+2\alpha)\frac{\Theta}{\omega}-1 \right]=0, \quad (2.18)$$

$$\omega^2-1+2\frac{\hbar-1}{M_{a1}^2}+\frac{5}{14M_1^2} \left\{ \left[\frac{2\gamma_{H_2}(1-\eta)}{(\gamma_{H_2}-1)}+10\eta+10\alpha \right] \Theta-7 \right\} + \frac{10}{7M_1^2} \left(\alpha\Theta_1^{ion} + \frac{\eta}{2}\Theta_1^{diss} \right) = 0. \quad (2.19)$$

It is necessary to add to them the chemical-equilibrium equation for dissociation, and the Saha equation for ionization:

$$\frac{\eta^2}{1-\eta} = \frac{g_H^2 \Omega^2}{16JN_1} \left(\frac{M}{\pi} \right)^{3/2} T_1^{-3/2} \omega \Theta^{-3/2} \exp\left(-\frac{\Theta_1^{diss}}{\Theta}\right), \quad (2.20)$$

$$\frac{\alpha^2}{1-\alpha} = \frac{2g_+}{g_H N_1} \left(\frac{2\pi m_e T_1}{h^2} \right)^{3/2} \omega \Theta^{3/2} \exp\left(-\frac{\Theta_1^{ion}}{\Theta}\right) \quad (2.21)$$

(J is the moment of inertia of the molecule). Simultaneous solution of these equations determines the boundary conditions. Figure 3 shows the temperature, density, and the degrees of ionization and dissociation behind the shock-wave front in hydrogen as functions of the Mach number M_1 .

For argon, we include in the boundary conditions the possibility of multiple ionization. We denote by g_s the statistical weight of the ground state of the s -fold ionized atoms, by Θ_s^{ion} the dimensionless potential of the s -th ionization, and by k the number of electrons in the atom. Taking electroneutrality into account, we reduce the Saha equation to the form

$$\alpha = \sum_{s=1}^k g_s \left[\frac{2}{N_1} \left(\frac{2\pi m_e T_1}{h^2} \right)^{3/2} \frac{\omega \Theta^{3/2}}{\alpha} \right]^s (s-\alpha) \exp\left(-\frac{1}{\Theta} \sum_{r=1}^s \Theta_r^{ion}\right). \quad (2.22)$$

Simultaneous solution of Eqs. (2.22) and (2.8)–(2.10), where the energy flow to the ionization (the last term of (2.3)) should be taken in the form

$$S_{ion} = \sum_{r=1}^k \sum_{s=1}^s I_r n_s u,$$

yields the values of the temperature, density, etc. behind the shock-wave front with allowance for multiple ionization. Figure 4 shows the temperature, density, and degree of ionization calculated in this manner as functions of M_1 for a shock wave in argon. We see that the single-ionization approximation alone is adequate up to the values $M_1=35$ (this limit shifts towards smaller values of M_1 if the initial density and the magnetic field are decreased).

3. STRUCTURE OF SHOCK-WAVE FRONT

The structure of the shock-wave front, i. e., the changes of the temperature, velocity, density, and magnetic field on going through the front, is completely determined by the system of equations (2.22)–(2.7), whose solutions differ with the relations between the rates of the dissipative processes and the ionization rate or, equivalently, with the relations between the characteristic scales of these processes. These scales are not universal as in the case of a fully ionized gas,^[3,9] but depend both on the actual gas and on its initial state. The qualitative character of the solutions obtained below, however, is common to all.

We consider two limiting cases in which the ionization rate in the shock wave is much smaller (or much larger) than the dissipation rate. The first case corresponds to the model of Zel'dovich and von Neumann: the shock wave consists of a narrow compression and heating zone (dissipation zone), which gives way to a much broader relaxation (ionization) zone. The dissipation in the relaxation zone is negligible, the density and the magnetic field vary slowly, and the temperature is decreased because of the energy lost to ionization.

In the opposite limiting case the ionization on the shock-wave front is quite rapid, so that local ionization equilibrium has time to be established over practically the entire width of the shock-wave front.

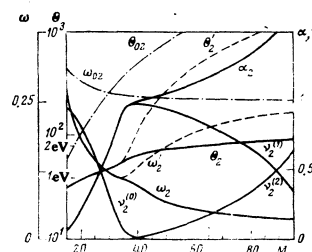


FIG. 4. Dimensionless temperature Θ , velocity ω , density ν , and degree of ionization α behind the shock-wave front in argon for $N_1=10^{16}$ cm $^{-3}$, $T_1=300$ K, and $\beta_1=0.1$ as functions of the Mach number M_1 . Dashed—the corresponding quantities without allowance for ionization, dash-dot—with allowance for only the first ionization.

Consider Mach numbers that are not too large, such that Δ_{ion} and Δ_{rec} in the state behind the front are much larger than all the other scales Δ_j , Δ_v , etc. For argon, e.g., at $\beta_1 = 1$ and $N_1 = 10^{17}$, this calls for $M_1 \lesssim 20$. Over the scales characteristic of the dissipation, we can then neglect ionization and recombination and put $\alpha = \alpha_1 = \text{const}$.

Let us compare the scales of the viscosity, thermal conductivity, and Joule dissipation. It is easily seen that for argon, for example, at $\beta_1 = 0.1$, in the region of initial densities $N_1 \sim 10^{16} - 10^{18}$ and Mach numbers $M_1 \lesssim 25$, the largest scale will be that of the Joule dissipation. We put $\Delta = \Delta_{j1}$; it follows then from (2.2) that

$$d\alpha/d\xi = O(\Delta_{j1}/\Delta_{ion}) \ll 1.$$

Thus, at $\Delta = \Delta_{j1}$ we have $\alpha = \alpha_1 \ll 1$. From (2.5) and (2.6), omitting the small terms, we obtain

$$\omega - 1 + \frac{3}{5M_1^2} \left(\frac{\Theta}{\omega} - 1 \right) + \frac{h^2 - 1}{2M_{a1}^2} = 0, \quad (3.1)$$

$$\omega^2 - 1 + \frac{3}{M_1^2} (\Theta - 1) + 2 \frac{h - 1}{M_{a1}^2} = 0. \quad (3.2)$$

The electron pressure in (3.2) we neglect, since $\alpha_1 \ll 1$. The electrons in the precursor layer in the heating zone are due to photoionization of the gas by radiation from the shock-wave front (see the Appendix). At the same time, because of the strong electronic thermal conductivity, the electron temperature changes little; the change of the temperature of the heavy particles by collisions with the electrons is also small, for at $\alpha_1 \ll 1$ we have $\Delta_r \gg \Delta_{j1}$. From (3.1) and (3.2) we get $h(\omega)$ and $\Theta(\omega)$:

$$h = \frac{1}{\omega} + \frac{3}{5\omega} \left\{ \left[1 + \frac{40M_{a1}^2}{9} (\omega - 1) (\omega_{02} - \omega) (\omega - \omega_{02-}) \right]^{1/2} - 1 \right\}, \quad (3.3)$$

$$\Theta = 1 - \frac{M_1^2}{3\omega} (\omega - 1) \left(\omega^2 + \omega - \frac{2}{M_{a1}^2} \right) - \frac{2M_1^2}{5M_{a1}^2 \omega} \times \left\{ \left[1 + \frac{40M_{a1}^2}{9} (\omega - 1) (\omega_{02} - \omega) (\omega - \omega_{02-}) \right]^{1/2} - 1 \right\}. \quad (3.4)$$

It is easily seen that h and Θ given by (3.3) and (3.4) satisfy the boundary conditions at the point 1, i.e., as $\xi \rightarrow -\infty$, where $\omega = h = \Theta = 1$. Equation (2.4) yields at $\Delta = \Delta_j$

$$h\omega - 1 = dh/d\xi. \quad (3.5)$$

Substituting (3.3) and (3.4) in (3.5) and putting $\Theta_e = \Theta_2$ (since the electron temperature varies little on the front and enters in the equation only in power-law fashion), we obtain the structure of the Joule-heating zone:

$$\xi - \xi_0 = \int_{(1+\omega_{02})/2}^{\cdot} \frac{dh}{d\omega'} \frac{d\omega'}{h\omega' - 1}. \quad (3.6)$$

The lower integration limit is chosen here such that $\omega(\xi_0) = (1 + \omega_{02})/2$. Expression (3.6) together with (3.3) and (3.4) yields the spatial variation of $h(\xi)$, $\omega(\xi)$ and $\Theta(\xi)$ from unity to their limiting values in the heating zone, which are determined from (3.1) and (3.2). At the end of the zone (state 02) the temperature then

reaches the maximum value $\Theta_{02}(\omega_{02})$, and $\omega = \omega_{02}$, $h = 1/\omega_{02}$. Behind the heating zone, the structure of the front is determined no longer by dissipation, but by ionization and recombination.

Putting $\Delta = \Delta_{ion}$ in (2.2)–(2.7) and recognizing that $\Theta = \Theta_e$ in this simplest case when $\Delta_{ion} \gg \Delta_r$, we obtain

$$d\alpha/d\xi = \alpha(1 - \alpha) - \alpha^3 \Delta_{rec}/\Delta_{ion}, \quad (3.7)$$

$$\omega - 1 + \frac{3}{5M_1^2} \left[\frac{\Theta}{\omega} (1 + \alpha) - 1 \right] + \frac{h^2 - 1}{2M_{a1}^2} = 0, \quad (3.8)$$

$$\omega^2 - 1 + \frac{3}{M_1^2} [\Theta(1 + \alpha) - 1] + 2 \frac{h - 1}{M_{a1}^2} + \frac{6\Theta_1^{ion}}{5M_1^2} \alpha = 0, \quad (3.9)$$

$$h\omega = 1. \quad (3.10)$$

The solution of Eqs. (3.7)–(3.10), which determines the structure of the relaxation zone, reduces to a single quadrature. The boundary conditions are specified in natural fashion: $\omega = \omega_{02}$, $h = 1/\omega_{02}$, $\Theta = \Theta_{02}$ and $\alpha = \alpha_1$ at the point 02 and $\omega = \omega_2$, $h = 1/\omega_2$, $\Theta = \Theta_2$ and $\alpha = \alpha_2$ behind the front at the point 2.

We note that at $\kappa \gtrsim 1$ it follows from (2.11) and (2.15) that the main change in the velocity, density, and magnetic field in an ionizing shock wave is concentrated in the relaxation zone. Owing to the large extent of the relaxation zone (compared with the heating zone) its structure can be observed directly with the aid of magnetic probes.

It was shown earlier^[3] that in a transverse shock wave the Joule dissipations may not be sufficient to realize a continuous solution. If the Alfvén Mach numbers exceed a certain critical value, an isomagnetic jump is produced on the shock-wave front. An analogous situation is possible in the heating zone. We rewrite (3.5) in the form

$$h\omega - 1 = \frac{dh}{d\omega} \frac{d\omega}{d\xi}. \quad (3.11)$$

Since it follows of necessity from the entropy-growth condition^[3] that $d\omega/d\xi < 0$ and $h\omega - 1 \geq 0$, we must stipulate satisfaction of the inequality

$$dh/d\omega \leq 0. \quad (3.12)$$

Consider $dh/d\omega$ at the limiting points of the heating zone. Ahead of the shock-wave front we have

$$(dh/d\omega)_1 = -M_{a1}^2 (1 - 1/M_1^2).$$

Rewriting (3.1) and (3.2) in terms of dimensionless variables referred to the values of the point 02, we obtain the same relation, except that the subscript 1 is replaced by 02 (M_{02} and M_{a02} are the Mach numbers at the point 02, and are connected with M_1 and M_{a1} as follows: $M_{02}^2 = M_1^2 \omega_{02}^2 / \Theta_{02}$, $M_{a02}^2 = M_{a1}^2 \omega_{02}^3$).

It is shown in^[3] that the necessary and sufficient condition for the absence of an isomagnetic jump is satisfaction of the inequalities $M_1^2 > 1$, $M_{02}^2 > 1$. Whereas the first of these inequalities is always satisfied, the second determines the level of the critical values of the Mach numbers (M_{a1} , M_1) above which a discontinuity appears in the zone of the Joule heating—the isomagne-

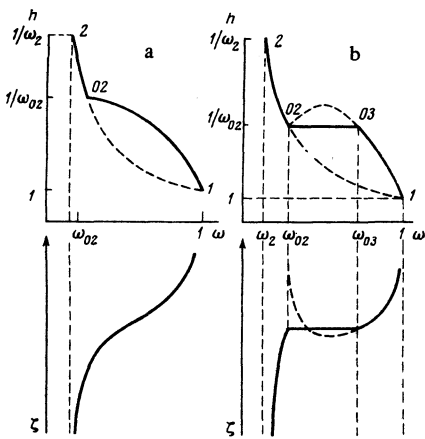


FIG. 5.

tic jump. Figure 5a shows the integral curves on the $h(\omega)$ and $\omega(\zeta)$ plane for a shock wave subcritical Mach numbers ($M_{02} < 1$). For the case $M_{02} > 1$ the same integral curves are shown in Fig. 5b. In the Joule-heating zone the velocity and the magnetic field change from unity at $\zeta = -\infty$ to $h = 1/\omega_{02}$ and $\omega = \omega_{03}$ at the start of the isomagnetic jump (we label this point with the subscript 03). The Joule-heating zone is replaced by an (03-02) isomagnetic jump—a gap with a width on the order of the mean free path. In the isomagnetic jump, the density and the temperature change from the initial values $1/\omega_{03}$ and ω_{03} to $1/\omega_{02}$ and ω_{02} . The isomagnetic jump is followed by a relaxation zone (02-2), whose structure is determined by Eqs. (3.7)–(3.10). The point 03 at which the isomagnetic jump begins can be easily obtained in terms of the Mach numbers M_{02} and M_{a02} , which in turn are expressed in terms of M_1 and M_{a1} (see above).

In fact, considering Eqs. (3.1) and (3.2) for variables referred to the point 02, and noting that h is constant from 02 to 03, we get

$$\omega_{03} = \frac{1}{8} \left\{ 5 + \frac{3}{M_{02}^2} - 5 \frac{h^2 - 1}{2M_{a02}^2} \pm \left[\left(5 + \frac{3}{M_{02}^2} - 5 \frac{h^2 - 1}{2M_{a02}^2} \right)^2 - 16 \left(1 + \frac{3}{M_{02}^2} - 2 \frac{h-1}{M_{a02}^2} \right) \right]^{1/2} \right\}, \quad (3.13a)$$

$$\Theta_{03} = 1 + \frac{M_{02}^2}{3} \left(1 - \omega_{03}^2 - 2 \frac{h-1}{M_{a02}^2} \right), \quad (3.13b)$$

where $h = 1/\omega_{02}$.

If the ionization is “frozen” (for example, in the case of a fully ionized plasma), the point 02 on the integral curve is the end point (i. e., the points 02 and 2 coincide). Then $h_{02} = h_2 = 1$ and Eqs. (3.13) go over into formulas (3.20) of [3], and it is this which determines the choice of the sign of the square root in (3.13a).

The structure of the isomagnetic jump is determined by the viscosity and by the thermal conductivity if the magnetic field is constant, i. e., this discontinuity is purely gasdynamic. The structure of the isomagnetic jump in a fully ionized plasma was investigated in [3], and the structure of gasdynamic shock waves in a weak-

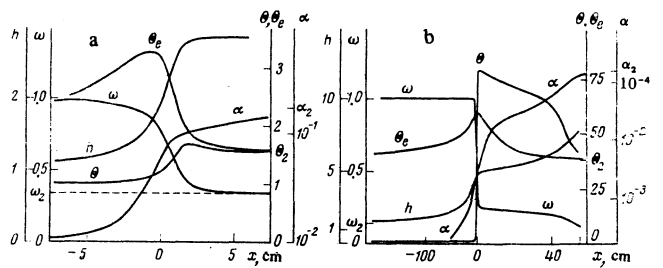


FIG. 6. Profiles of shock waves in argon, obtained by numerically solving the system of initial equations: a) $M < M_{cr}$, b) $M > M_{cr}$.

ly ionized plasma was investigated in [13].

Figure 6 shows the changes of the temperature, velocity, and magnetic field in a shock wave in argon with allowance for single ionization. Figure 6a shows a shock wave with subcritical Mach number, when all the heating is due only to Joule dissipations. In Fig. 6b the Mach numbers are higher than critical. The heating in the isomagnetic jump is due to viscosity and thermal conductivity. The temperature behind the front increases with increasing shock-wave intensity, and the ionization length decreases exponentially, i. e., the relaxation zone becomes thinner. In final analysis, the ionization scale becomes substantially smaller than the scale of the Joule dissipations. The shock-wave front can then no longer be subdivided into the compression and ionization zones. The heating on the front of the shock wave is accompanied throughout by simultaneous ionization, and then at $\Delta_j \gg \Delta_{ion}$ and $\Delta_j \gg \Delta_{rec}$ the degree of ionization is locally in equilibrium and is determined by the Saha formula.

To determine the structure of the shock wave, we turn in this case, too, to Eqs. (2.3)–(2.7), referring the dimensionless variables to the state behind the shock-wave front. It suffices for this purpose to interchange the indices, $1 \leftrightarrow 2$. The resultant Mach numbers M_2 and M_{02} are simply connected with M_1 and M_{a1} :

$$M_2^2 = \omega_2^2 M_1^2 / (1 + \alpha_2) \Theta_2, \quad M_{a2}^2 = \omega_2^2 M_{a1}^2.$$

The Mach-number (M_2 , M_{a2}) variation region corresponding to the shock wave is shown in Fig. 7.

Putting $\Delta = \Delta_j$ in (2.3)–(2.7) and recognizing that $\Delta_{j2} \gg \Delta_v, \Delta_T, \Delta_{ion}, \Delta_{rec}$, we get

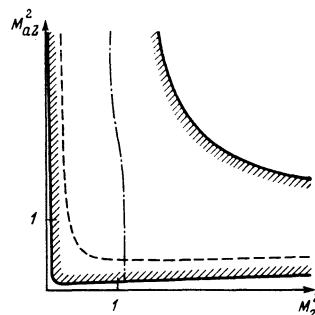


FIG. 7. Region in which the Mach numbers M_2^2 and M_{a2}^2 vary and which corresponds to the shock wave. The dashed line is a plot of $M_2^2 = M_{2cr}^2$.

$$\frac{\alpha^2}{1-\alpha} = \frac{\alpha_2^2}{1-\alpha_2} \omega \Theta^{1/2} \exp\left(\Theta_2^{ion} - \frac{\Theta_2^{ion}}{\Theta}\right), \quad (3.14)$$

$$h\omega - 1 = dh/d\xi, \quad (3.15)$$

$$\omega - 1 + \frac{3}{5M_2^2(1+\alpha_2)} \left[(1+\alpha) \frac{\Theta}{\omega} - 1 - \alpha_2 \right] + \frac{h^2 - 1}{2M_{\alpha_2}^2} = 0, \quad (3.16)$$

$$\omega^2 - 1 + \frac{3}{M_2^2(1+\alpha_2)} \left[(1+\alpha)\Theta - 1 - \alpha_2 \right] + 2 \frac{h-1}{M_{\alpha_2}^2} + \frac{6\Theta_2^{ion}}{5M_2^2(1+\alpha_2)} (\alpha - \alpha_2) = 0. \quad (3.17)$$

With the aid of the system of transcendental equations (3.14), (3.16) and (3.17) we can express α , Θ , and h in terms of ω , after which the system (3.14)–(3.17) reduces to a single quadrature (3.15).

In this case, too, the Joule dissipations may turn out to be insufficient for a continuous transition from point 1 to point 2. To find the conditions for the appearance of an isomagnetic jump and the critical Mach numbers, we calculate $dh/d\omega$ at the point 2. From (3.14), (3.16), and (3.17), taking into account the boundary conditions at the point 2 for Eqs. (3.14)–(3.17) ($\omega(2) = h(2) = \Theta(2) = 1$, $\alpha(2) = \alpha_2$), we get

$$\frac{1}{M_{\alpha_2}^2} \left(\frac{dh}{d\omega} \right)_2 = \frac{1}{M_2^2} - 1 - \frac{4\alpha_2(1-\alpha_2)(\Theta_2^{ion})^2}{15M_2^2(1+\alpha_2)(2-\alpha_2)} \left[1 + \left(\frac{3}{2} + \Theta_2^{ion} \right)^2 \frac{2\alpha_2(1-\alpha_2)}{3(1+\alpha_2)(2-\alpha_2)} \right]^{-1}. \quad (3.18)$$

The critical value of M_2^2 is therefore

$$M_{2cr}^2 = 1 - 4 \left[\frac{15(1+\alpha_2)(2-\alpha_2)}{\alpha_2(1-\alpha_2)(\Theta_2^{ion})^2} + 10 \left(1 + \frac{3}{2\Theta_2^{ion}} \right)^2 \right]^{-1}. \quad (3.19)$$

At $M_2^2 > M_{2cr}^2$ the structure of the shock-wave front is determined entirely by the Joule dissipations; typical integral curves on the plane $h(\omega)$ and $\omega(\xi)$ are shown in Fig. 8a (these shock waves correspond to Mach numbers M_2^2 and $M_{\alpha_2}^2$ in the region to the right of the dashed line $M_2^2 = M_{2cr}^2$ on the $(M_2^2, M_{\alpha_2}^2)$ plane of Fig. 7). On the other hand if $M_2^2 < M_{2cr}^2$, then an isomagnetic jump appears in the structure of the shock-wave front. The plots of $h(\omega)$ and $\omega(\xi)$ are in this case the same as shown in Fig. 8b.

The start of the isomagnetic jump, i. e., $\omega_{03}(M_2)$, $\Theta_{03}(M_2)$, α_{03} , is determined by solving Eqs. (3.14), (3.16), and (3.17), in which we must put $h=1$. The

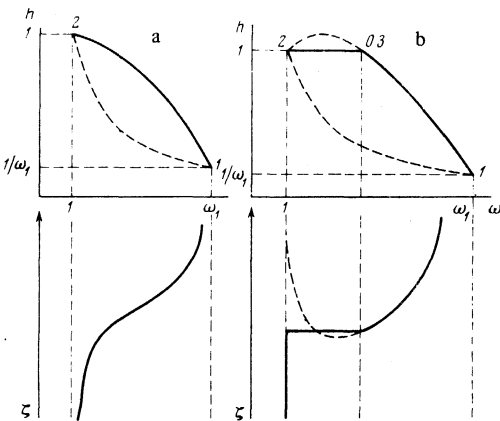


FIG. 8.

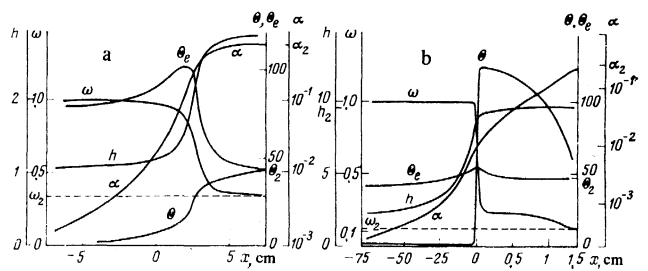


FIG. 9. Shock-wave profiles in argon, obtained by numerically solving the system of initial equations: a) at $M_2^2 > M_{2cr}^2$, b) at $M_2^2 < M_{2cr}^2$.

structure of the isomagnetic jump is determined both by the viscosity and thermal conductivity, and by the ionization kinetics. It is described by Eqs. (2.3)–(2.7) in dimensionless variables referred to the state 2, and we must put $h=1$ in these variables. Solutions for hydrodynamic discontinuities of this type were investigated in^[17]. We note here also other papers^[18–20] devoted to attempts at determining the structure of an ionizing shock wave in a magnetic field.

Figures 9a and 9b show the changes of the velocity, density, and magnetic field, obtained by numerically solving the initial equations for shock waves that have no relaxation zones. On Fig. 9a we have $M_2^2 > M_{2cr}^2$, and there are no internal discontinuities. On Fig. 9b, we have $M_2^2 < M_{2cr}^2$ and an isomagnetic jump appears in the front structure.

Petschek and Byron^[5] and Mamimoto and Teshima^[6] measured the width of the relaxation zone of a shock wave in argon without a magnetic field at different values of the initial pressure. The experimentally measured quantity τ is the ionization growth time. If $\Delta_{ion}(2) = u_1 \omega_2^2 / N_1 \alpha_{ion}(2)$ is the characteristic ionization length (see Eq. (3.7)), then

$$\tau = \Delta_{ion}(2) / u_2 = \omega_2 / N_1 \alpha_{ion}(2).$$

A convenient parameter is the quantity p_1 , which depends little on the initial pressure p_1 ($T_1 = 300$ K):

$$p_1 \tau = T_1 \omega_2 / \alpha_{ion}(2). \quad (3.20)$$

Figure 10, taken from the paper of Makimoto and Teshima,^[6] shows a plot of $p_1 \tau$ vs. the reciprocal temperature behind the shock-wave front in argon, calculated without allowance for ionization; the dashed line shows the values calculated by formula (3.20) for $p_1 = 2$ Torr.

4. BOUNDARY CONDITIONS. COMPARISON WITH EXPERIMENT

It follows from (2.4) that in the rest system of the gas the vanishing of the derivative of the magnetic field far ahead of the shock-wave front is due either to the absence of an electric field or to zero conductivity of the gas ($\sigma_1 = 0$). Formally, an arbitrarily small value of σ_1 leads to the absence of current as $x \rightarrow -\infty$, and consequently to the absence of an electric field in the

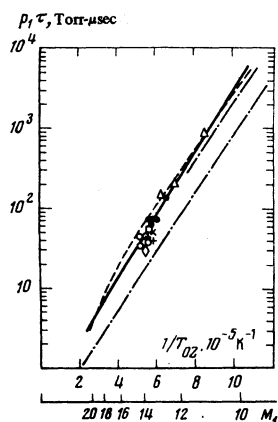


FIG. 10. Time of ionization relaxation as a function of the reciprocal temperature. The experimental points and the dash-dot and solid lines are the results of measurements and numerical calculations gathered in [6]. The dashed line is obtained by calculation with formula (3.20).

rest system of the gas. This raises the question of how small σ_1 must be to be able to assume $\sigma_1 = 0$. This question has led to a number of obscurities, for if $\sigma_1 = 0$ exactly, the condition $E_{y1} = u_1 H_1 / c$ need not necessarily be satisfied, and an electric field can exist ahead of the wave front in the rest system of the gas. The conservation equations are therefore insufficient for a determination of the boundary conditions.

Consider the dispersion equation for the propagation of small oscillations across a magnetic field in a medium with finite conductivity:

$$k^2 \tilde{u}_s^2 - \omega^2 + \frac{i}{2} (k\delta)^2 \times \left(1 - \frac{\omega^2}{k^2 c^2} \right) (k^2 u_s^2 - \omega^2) = 0, \quad (4.1)$$

where u_s is the speed of sound, $\tilde{u}_s = (u_s^2 + u_a^2)^{1/2}$ is the fast magnetic sound, and $\delta = c / (2\pi\sigma_1\omega)^{1/2}$ is the skin depth. At $(k\delta)^2 \gg 1$, Eq. (4.1) describes the propagation of acoustic and electromagnetic waves with small resistive damping in terms of $(k\delta)^{-2}$ in the inverse case $(k\delta)^2 \ll 1$, Eq. (4.1) describes magnetosonic oscillations with a damping small relative to $(k\delta)^2$.

We assume $k = 1/\Delta$ and $\omega = u_1/\Delta$, where Δ is the considered length scale and u_1 is the velocity in the incoming flow. Then

$$\frac{1}{2} (k\delta)^2 = \frac{c^2}{4\pi\sigma_1 u_1 \Delta} = \frac{\Delta_{j1}}{\Delta}, \quad (4.2)$$

where Δ_{j1} is the Joule scale introduced above (the magnetic-field diffusion length).

Thus, over scales $\Delta \gg \Delta_{j1}$ we have ordinary hydrodynamics, and at $\Delta \ll \Delta_{j1}$ the situation is the same as if $\sigma_1 = 0$. The limit $\sigma_1 \rightarrow 0$ means an infinite increase of the scale over which the situation can be regarded as magnetohydrodynamic. The "true initial state" corresponding to the absence of an electric field in the rest system of the gas and to magnetohydrodynamic boundary conditions is reached far (on the order of several times Δ_{j1}) from the region of the viscous density jump. The transition to this point corresponds to small gradients and cannot be observed if the apparatus dimensions are smaller than Δ_{j1} .

It is obvious that the precursor ionization (which is external with respect to the hydrodynamic model) is significant from the point of view of the observed magnetic structure of the shock wave.^[4] In a transverse shock wave, where the diffusion of the hot electrons is hindered, the precursor ionization is the result of photoionization of the incident stream by the radiation coming from the hot gas on account of the shock-wave front. For monatomic gases, an important role is played by the two-step process of absorption of the resonance line and the subsequent ionization of the excited atoms by the radiation of the continuum.^[21,22] At the same time, for the hydrogen used in the experiment of^[4], it suffices to assume by way of estimate that the radiation flux is proportional to the black-body radiation flux with a temperature equal to the temperature T_2 behind the front. Assuming that the degree of ionization α_1 is proportional to the absorbed radiation flux and neglecting the slow variation of the density ahead of the wave front, we obtain

$$\alpha_1(x) = \alpha_0 \exp\left(\frac{x}{l_p}\right), \quad \alpha_0 \propto \frac{T_2}{u_1} \exp\left(-\frac{I}{T_2}\right),$$

where $l_p = 1/N_1\sigma_p$ is the range of the ionizing quanta in the gas ahead of the front (see the Appendix).

Stebbins and Vlases,^[4] using a setup with an inverse Z-pinch, investigated the structure of a transverse ionizing shock wave. Comparing the experimental results with the theory (see^[7,8]), these authors point out to a substantial discrepancy between the measurement of the electric field behind the front and the theoretical calculations. Another contradiction must also be pointed out: whereas according to the theory^[7,8] the pressure pulse (the density jump) should occur ahead of the change of the magnetic field, the oscillograms of^[4] show that the pressure pulse always follows the change of the magnetic field.

These contradictions disappear if the structure of the shock wave is described in accordance with the theory developed above. Calculation of the values of Δ_j and Δ_{10n} for the shock waves investigated in^[4] shows that they are moderately strong, i. e., the ionization is negligibly small in the heating zone, and the structure of the magnetic field is the same as shown in Figs. 5a and 5b. According to the the oscillogram shown in Fig. 5 of the paper of Stebbins and Vlases,^[4] it should be assumed that the magnetic and electric fields are measured not behind the shock-wave front, but in the region of the Joule dissipations ahead of the isomagnetic jump. From the oscillogram of the magnetic field ahead of the shock-wave front it is seen that the faster waves propagate through the gas with the larger conductivity, although the gas was not pre-ionized in the experiments of^[4].

As seen from Figs. 5b, the change of the magnetic field near the point 03 can be appreciable, of the order of $1/\omega_{02}$, whereas the electric field in this point is small if the main velocity jump takes place in the isomagnetic jump, and $u_1/u_{03} \approx 1$. Near the point 03 (Fig. 5b) we have ahead of the isomagnetic jump

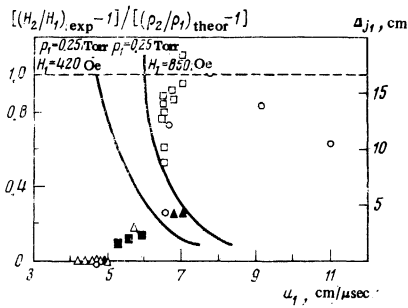


FIG. 11.

$$H_{02}/H_1 = H_{02}/H_1 = u_1/u_{02}, \quad (4.3)$$

$$E_{03}^* = \frac{u_1 H_1}{c} \left(1 - \frac{u_{03}}{u_1}\right) \left(\frac{u_1}{u_{02}}\right).$$

For a concrete comparison of the theory with experiment, let us examine the Stebbins and Vlases^[4] data on the strongest shock waves, characterized by the largest values of M_{01} (i. e., for the maximal initial pressure $p_1 = 250$ mm Hg and minimal magnetic fields H_1 equal to 420 and 850 Oe). Estimates show that the stationary width of the weaker waves is larger than the dimensions of the installation, i. e., shock waves with smaller values of M_{01} do not manage to assume the stationary values in the experiments of^[4]. A theoretical interpretation of such results is difficult. Figure 11, taken from^[4], shows a plot of Δ_{j1} against the shock-wave velocity u_1 . It is seen that the transition observed in^[4] from the ordinary hydrodynamic regime to the magnetohydrodynamic one of the changes of the magnetic field in the shock wave takes place precisely when the scale of the variation of the magnetic field ahead of the viscous jump Δ_{j1} becomes less than the dimensions of the installation.

Table I lists the values of M_{01} , M_{02} , h_2 , h_{03} , Δ_{j1} , and E_{03}^* calculated from the formulas given above, and also the measured values of H_2/H_1 and E_{03}^* . It is seen that the results of the experiment agree well with the theory, and the agreement is better the small Δ_{j1} in comparison with the dimension of the installation.

The authors thank L. P. Pitaevskii for useful discussions.

APPENDIX. PHOTOIONIZATION IN THE PRECURSOR LAYER

Let us estimate the concentration and the temperature of the photoionization electrons in the incoming stream ahead of the shock-wave front. Assume that the hot gas behind the shock-wave front radiates like a black body with temperature $T_2 \ll I$ (I is the ionization potential). For the flux density of the quanta having a frequency in the interval $d\omega$ we have

$$dS_p = \frac{\omega^2 d\omega}{4\pi^2 c^2} \left[\exp\left(\frac{\hbar\omega}{T_2}\right) - 1 \right]^{-1}.$$

The flux density of the ionizing photons with energy $\hbar\omega \geq I$, which leave the shock layer, is given, accurate

to small terms of order T_2/I , by

$$S_p = \int_{(I/\hbar)}^{\infty} \frac{dS_p}{d\omega} d\omega = \frac{I^2 T_2}{4\pi^2 c^2 \hbar^3} \exp\left(-\frac{I}{T_2}\right). \quad (A.1)$$

In the stationary case, the balance equation for the electrons is

$$u_1 \frac{dn_e}{dx} = S_p N_a \sigma_p \exp\left(\frac{x}{l_p}\right) - \beta_{rec} n_e^3, \quad (A.2)$$

where σ_p is the photoionization cross section and β_{rec} is the three-particle recombination coefficient. Comparing the rate at which the electrons flow into the shock layer and the rate at which they depart by recombination, we find that the recombination is small if

$$N_a \ll u_1 \sigma_p / \beta_{rec} \alpha^2. \quad (A.3)$$

Substituting the numerical values of β_{rec} and σ_p for hydrogen, we get

$$N_a \ll \frac{10^{15}}{\alpha^2} \left(\frac{u_1}{10^8}\right) \left(\frac{T_2}{10^4 \text{ K}}\right)^{3/2}.$$

Thus, for the customarily encountered values of the gas density, the recombination in the precursor layer is insignificant. Omitting the last term of (A.2), we obtain for the electron density in the precursor layer

$$n_e = \frac{S_p}{u_1} \exp\left(\frac{x}{l_p}\right), \quad (A.4)$$

where $l_p = 1/N_a \sigma_p$ is the mean free path of the ionizing quanta.

We estimate now the electron temperature in the precursor layer. The flux density of the quanta whose energy is in the interval δE is

$$\delta S_p = \frac{1}{4\pi^2 c^2 \hbar^3} E^2 \delta E \exp\left(-\frac{E}{T_2}\right).$$

We denote the energy of the produced photoelectron by $\varepsilon = E - I$, and we assume for the photoionization cross section

$$\sigma_p = \begin{cases} 0, & E < I, \\ \text{const}, & E \geq I. \end{cases}$$

From the electron balance equation we obtain

$$u_1 \delta n_e = N_a \sigma_p \delta S_p(E), \quad (A.5)$$

hence the average electron density in the precursor

TABLE I.

H_1 , Oe	u_1 , cm/ μ sec	M_{01}	M_{02}	$h_{02} = \frac{H_{02}}{H_1}$	$\left(\frac{H_2}{H_1}\right)_{\text{exp}}$	E_{03}^* , V/cm	$E_{03}^* \text{exp}$, V/cm	Δ_{j1} , cm
420	5.90	8.2	0.46	4.4	{ 2.10 3.08	16	{ 13 14	6
	6.55	9.1	0.45	4.3	{ 4.93 5.50	14	{ 14 16	3
850	5.75	3.9	0.70	3.6	{ 1.63	91	{ 34 56	31
	6.55	4.5	0.62	3.7	{ 4.37 4.19	85	{ 56 50	8

layer ahead of the shock-wave front is

$$\langle \delta n_e \rangle = \frac{N_a}{u_1} \int_0^\infty \sigma_p \delta S_p(E) = \frac{I^2 T_2 N_a}{4\pi^2 c^2 h^3 u_1} \exp\left(-\frac{I}{T_2}\right).$$

Multiplying (A. 5) by ε and integrating, we obtain for the average energy

$$\langle \varepsilon \rangle = \langle \varepsilon \delta n_e \rangle / \langle \delta n_e \rangle = T_2.$$

If at the same time the scale of the electron-temperature relaxation is large in comparison with l_p , then the temperature of the electrons in the precursor layer is constant. The last condition takes the form

$$\frac{M_1}{\varepsilon} \frac{\sigma_p \theta_e^{-1/2}}{\alpha_1 \sigma_{ei} + (1 - \alpha_1) \sigma_{ea}} \gg 1. \quad (\text{A. 6})$$

Substituting in (A. 6) the values of the cross sections for real gases and assuming that $\alpha_1 \lesssim 10^{-2} - 10^{-3}$, we easily verify that (A. 6) is satisfied for all the gases at $M_1 \gtrsim 20$.

¹⁾ A similar situation obtains for the jump of the potential through the front of a shock wave in a plasma (see^[3,9]).

²⁾ To express in unified manner the transport coefficients in terms of cross sections averaged over the Maxwell distributions, we shall approximate below the average of the product by the product of the average values (e. g., $\langle \sigma v \rangle = \langle \sigma \rangle \langle v \rangle$ in the expression for the collision frequency). In this approximation, the qualitative $\sigma(v)$ dependence is apparently sufficiently well accounted for for comparison with experiment.

³⁾ It should be noted that an analogous interpolation in^[13] underestimates by a factor of two or three the cross section in

comparison with the experimental data.^[14]

- ¹C. K. Chu and R. Gross, Shock waves in plasma physics, Russ. transl. in: Fizika vysokotemperaturnoi plazmy (Physics of High-Temperature Plasma), M. S. Rabinovich, ed., Mir, 1972.
- ²R. Gross, Physics of strong shock waves in gases, Russ. transl. in: Fizika vysokikh plostonostei energii (Physics of High Energy Densities), O. N. Krokhin, ed., Mir, 1974.
- ³A. L. Velikovich and M. A. Liberman, Zh. Eksp. Teor. Fiz. **71**, 1390 (1976) [Sov. Phys. JETP **44**, 727 (1976)].
- ⁴C. F. Stebbins and G. C. Vlases, J. Plasma Phys. **2**, 633 (1968).
- ⁵H. Petschek and S. Byron, Ann. Phys. (N. Y.) **1**, 270 (1957).
- ⁶G. Kamimoto and K. Teshima, Transactions of the Japan Soc. for Aeronautical and Space Science **15**, No. 29, 124 (1972).
- ⁷A. G. Kullikovskii and G. A. Lyubimov, Dokl. Akad. Nauk SSSR **129**, 525 (1959) [Sov. Phys. Dokl. **4**, 1195 (1960)].
- ⁸C. K. Chu, Phys. Fluids **7**, 1349 (1964).
- ⁹A. L. Velikovich and M. A. Liberman, Fiz. Plazmy **2**, 334 (1976) [Sov. J. Plasma Phys. **2**, 182 (1976)].
- ¹⁰H. D. Weymann, Phys. Fluids **3**, 545 (1960).
- ¹¹T. G. McRae and B. M. Leadon, Phys. Fluids **15**, 2067 (1972).
- ¹²E. J. Morgan and R. D. Morrison, Phys. Fluids **8**, 1608 (1965).
- ¹³M. Y. Jaffrin, Phys. Fluids **8**, 606 (1965).
- ¹⁴L. J. Kieffer, Atomic Data **2**, 293 (1971).
- ¹⁵S. I. Braginskii, Voprosy teorii plazmy (Problems of Plasma Theory), Vol. 1, Atomizdat, 1963.
- ¹⁶S. Chapman and T. G. Cowling Mathematical Theory of Non-Uniform Gases, Cambridge Univ. Press, 1970.
- ¹⁷D. L. Chubb, Phys. Fluids **11**, 2363 (1968).
- ¹⁸M. I. Hoffert, Phys. Fluids **11**, 77 (1968).
- ¹⁹B. P. Leonard, J. Plasma Phys. **11**, 51 (1974).
- ²⁰B. P. Leonard, J. Plasma Phys. **7**, 133 (1972).
- ²¹W. H. Foley and J. H. Clarke, Phys. Fluids **16**, 375 (1973).
- ²²H. F. Nelson, Phys. Fluids **16**, 2132 (1973).

Translated by J. G. Adashko